

# Biochemical Basis of Oxidative Protein Folding in the Endoplasmic Reticulum

Benjamin P. Tu,\* Siew C. Ho-Schleyer,\* Kevin J. Travers,  
Jonathan S. Weissman†

The endoplasmic reticulum (ER) supports disulfide bond formation by a poorly understood mechanism requiring protein disulfide isomerase (PDI) and Ero1. In yeast, Ero1p-mediated oxidative folding was shown to depend on cellular flavin adenine dinucleotide (FAD) levels but not on ubiquinone or heme, and Ero1p was shown to be a FAD-binding protein. We reconstituted efficient oxidative folding in vitro using FAD, PDI, and Ero1p. Disulfide formation proceeded by direct delivery of oxidizing equivalents from Ero1p to folding substrates via PDI. This kinetic shuttling of oxidizing equivalents could allow the ER to support rapid disulfide formation while maintaining the ability to reduce and rearrange incorrect disulfide bonds.

Proteins that traverse the secretory pathway are typically stabilized by one or more disulfide bonds. To support efficient disulfide formation, cells actively promote oxidation in the two compartments where disulfide-linked folding commonly occurs: the eukaryotic ER (1) and the bacterial periplasm (2). In bacteria, an electron transport pathway links disulfide bond formation to the respiratory chain (3, 4). The integral membrane protein DsbB oxidizes the CxxC active site of the PDI homolog DsbA, which then catalyzes disulfide formation in folding proteins. DsbB is reoxidized by ubiquinone produced during respiration.

Over the past few decades, a number of factors have been suggested to contribute to disulfide formation in the ER, including secretion of reduced thiols, uptake of oxidized thiols, and a variety of redox enzymes and small-molecule oxidants (1, 5, 6). The physiological importance of any of these to disulfide formation has not been established. Genetic studies in *Saccharomyces cerevisiae* have identified an essential and conserved ER-resident protein, Ero1p (7, 8), the loss of which results in the accumulation of reduced PDI and the cessation of disulfide bond formation. Although this phenotype resembles that resulting from the loss of DsbB in bacteria (9), Ero1p has no apparent homology to DsbB or any other redox enzymes. Thus, whether oxidative folding occurs by a similar biochemical mechanism in eukaryotes and bacteria, or even whether Ero1p can catalyze redox reactions, is not known.

To define the requirements for oxidative

folding in the ER, we used reverse genetics in *S. cerevisiae* to eliminate components of the cellular redox machinery and examined the effects on disulfide-linked folding. We monitored disulfide formation by pulsing cells with the reductant dithiothreitol (DTT) and by monitoring the rate and efficiency of folding of newly synthesized carboxypeptidase Y (CPY), which contains five disulfide bonds required for folding and ER export (10). Deletion of *COQ5* or *HEM1*, which blocks biosynthesis of ubiquinone (11, 12) or heme (13), respectively, inhibited respiration and ER-associated cytochromes but did not alter the kinetics of CPY folding (Fig. 1A). Depletion of Nfs1p, an essential protein required for iron-sulfur (Fe-S) cluster assembly (14), also had little effect on CPY folding (Fig. 1A) (15). Moreover, under depletion conditions where the activities of known Fe-S cluster proteins are abolished (14), the kinetics of Ero1p reoxidation were comparable to those of a wild-type strain (Fig. 1B). Finally, Ero1p was functional in yeast grown under strictly anaerobic conditions (15). Thus, Fe-S clusters, molecular oxygen, ubiquinone, and hemes are not required for Ero1p-mediated oxidative folding.

We then investigated the role of riboflavin and its metabolic derivatives [flavin mononucleotide (FMN) and flavin adenine dinucleotide (FAD)] in oxidative folding using a strain lacking the *RIB5* gene, which is required for riboflavin biosynthesis. Depletion of riboflavin from the growth media inhibited CPY folding in a  $\Delta rib5$  strain (Fig. 1A) and caused PDI (16) and Ero1p to accumulate in a reduced form, even in the absence of DTT (Fig. 1B). Depletion of riboflavin also results in loss of FMN and FAD, which are derived from the sequential activities of Fmn1p and Fad1p, respectively (17). To determine whether these components are important for Ero1p-mediated folding, we examined the effect of

overexpression of *FMN1* or *FAD1* on a strain containing a temperature-sensitive allele of *ERO1* (*ero1-1*) (8). Overexpression of *FMN1* led to a modest enhancement of *ero1-1* viability, whereas overexpression of *FAD1* strongly suppressed the *ero1-1* temperature-sensitive phenotype (Fig. 1C). Moreover, addition of FAD to microsomes derived from wild-type but not *ero1-1* yeast greatly accelerated both the rate and yield of PDI reoxidation after DTT treatment (Fig. 1D); this finding strongly implies a direct role of FAD in disulfide bond formation. Taken together, our results indicate that Ero1p-mediated oxidative folding is exquisitely sensitive to cellular FAD levels.

To directly assess the biochemical mechanism of oxidative folding, we developed an affinity-based purification that yielded highly purified polyoma epitope-tagged Ero1p (Ero1p-Py<sub>2</sub>) from yeast microsomes (15) (Fig. 2A). Because further purification of Ero1p-Py<sub>2</sub> using anti-polyoma resin did not alter its activities in subsequent analyses, our Ero1p preparations likely contained no functional contaminants (16). Purified Ero1p displayed a distinct absorbance peak at 450 nm (16). Reversed-phase high-performance liquid chromatography (rpHPLC) analysis of denatured Ero1p revealed a single fluorescence peak that coeluted with a FAD standard (Fig. 2B). Thus, Ero1p itself is a flavoprotein that contains noncovalently bound FAD.

We next asked whether Ero1p could act as an oxidase in vitro by monitoring its activity on a well-characterized folding substrate, ribonuclease A (RNase A), which contains four disulfides necessary for its folding and activity (18). In the presence of supplemental FAD and PDI, catalytic amounts of Ero1p rapidly promoted the reactivation of reduced RNase A (Fig. 3A). SDS-polyacrylamide gel electrophoresis (PAGE) analysis directly demonstrated that the reactivation of RNase A resulted from Ero1p-mediated reoxidation of its four disulfide bonds (Fig. 3B). The observed refolding of RNase A was completely dependent on Ero1p, PDI, and supplemental FAD, but it did not require reduced (GSH) or oxidized (GSSG) glutathione, nor was it affected by pyridine nucleotide cofactors [e.g., nicotinamide adenine dinucleotide (NAD<sup>+</sup>) or the reduced form of NAD<sup>+</sup> phosphate (NADPH)] (15). There was also a strong preference for FAD over FMN (15), in agreement with in vivo observations (Fig. 1C). Increasing concentrations of Ero1p enhanced the rate of RNase A oxidative refolding (Fig. 3A). Even at a stoichiometry of one Ero1p molecule per 340 RNase A disulfide bonds, refolding proceeded at a rate that was significantly faster than the refolding of RNase A in the presence of PDI and an optimal glutathione redox buffer (Fig. 3A). Moreover, an Ero1p mutant that is nonfunc-

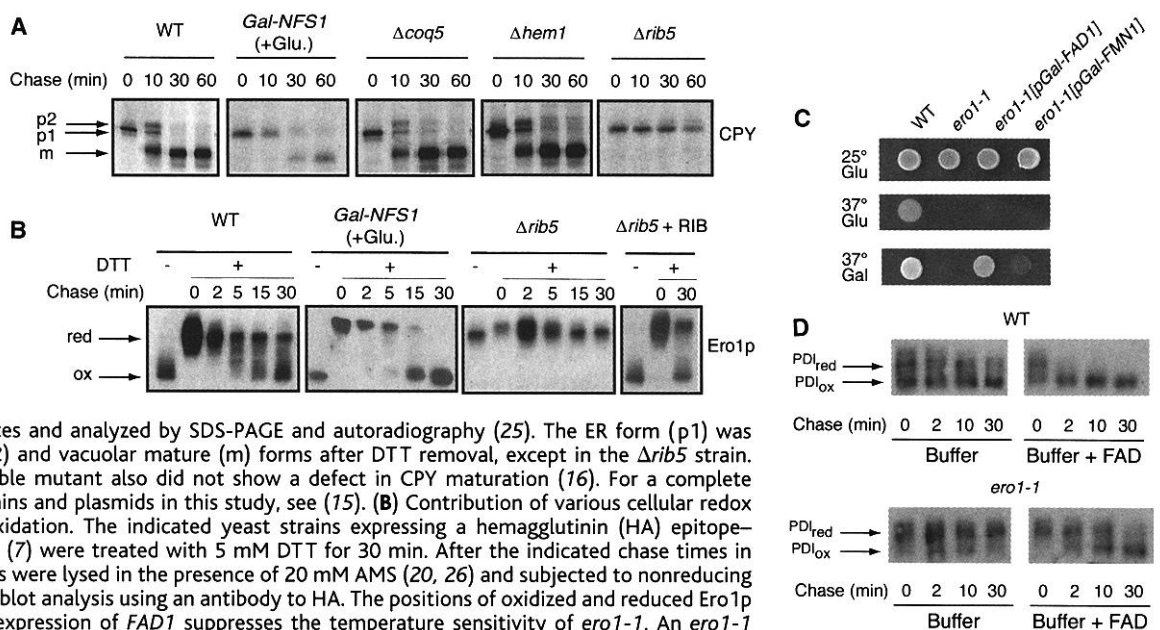
Howard Hughes Medical Institute, Department of Cellular and Molecular Pharmacology, University of California, San Francisco, CA 94143, USA.

\*These authors contributed equally to this report.

†To whom correspondence should be addressed. E-mail: jsw1@itsa.ucsf.edu

REPORTS

**Fig. 1.** Oxidative protein folding is highly sensitive to cellular FAD levels. **(A)** Contribution of various cellular redox cofactors to oxidative folding of CPY. The indicated yeast strains were labeled with [<sup>35</sup>S]methionine for 7 min in the presence of 5 mM DTT, and then chased in the absence of DTT for the indicated times. CPY was immunoprecipitated from cell lysates and analyzed by SDS-PAGE and autoradiography (25). The ER form (p1) was chased to the Golgi (p2) and vacuolar mature (m) forms after DTT removal, except in the  $\Delta rib5$  strain. The  $\Delta coq5 \Delta hem1$  double mutant also did not show a defect in CPY maturation (16). For a complete description of yeast strains and plasmids in this study, see (15). **(B)** Contribution of various cellular redox cofactors to Ero1p reoxidation. The indicated yeast strains expressing a hemagglutinin (HA) epitope-tagged version of Ero1p (7) were treated with 5 mM DTT for 30 min. After the indicated chase times in the absence of DTT, cells were lysed in the presence of 20 mM AMS (20, 26) and subjected to nonreducing SDS-PAGE and Western blot analysis using an antibody to HA. The positions of oxidized and reduced Ero1p are indicated. **(C)** Overexpression of *FAD1* suppresses the temperature sensitivity of *ero1-1*. An *ero1-1* strain carrying a vector with no insert, or an insert encoding *FMN1* or *FAD1* regulated by the *GAL1* promoter (pGal-*FMN1* or pGal-*FAD1*, respectively) (15), or an isogenic *ERO1* [wild-type/(WT)] strain carrying an empty vector were spotted on media containing glucose at 25°C, glucose at 37°C, or galactose at 37°C. **(D)** FAD induces reoxidation of PDI in microsomes. Microsomes from WT and *ero1-1* yeast were treated with DTT and incubated in buffer lacking DTT with or without 200  $\mu$ M FAD for the indicated times. Samples were then subjected to AMS modification, SDS-PAGE, and Western blot analysis using an antibody to PDI (27). Addition of GSSG also induced reoxidation of PDI, in an Ero1p-independent manner (15).



tional *in vivo* (16, 19) could not catalyze reoxidation of RNase A (Fig. 3, A and B). Thus, Ero1p is an efficient oxidase that catalyzes *de novo* disulfide bond formation through a FAD-dependent mechanism.

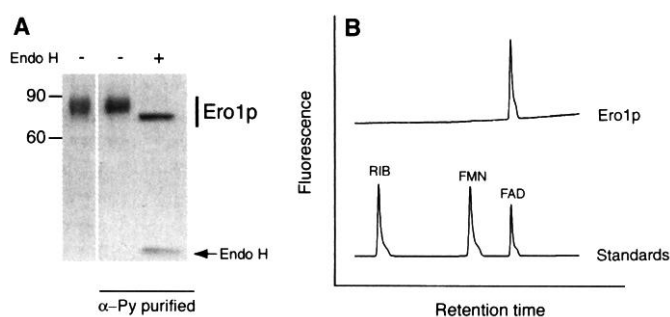
In the absence of PDI, folding substrates remained reduced *in vitro* (Fig. 3, A and B) and *in vivo* (20), even with Ero1p present. This finding suggests that PDI acts as an intermediary in the disulfide formation process by transferring oxidizing equivalents derived from Ero1p to folding substrates. We examined whether a mutant PDI in which the second cysteine of both active sites is changed to alanine [PDI (CxxA)<sub>2</sub>] could support Ero1p-mediated oxidative refolding of RNase A. This mutant PDI retains disulfide isomerase activity but cannot function as an oxidase (21). Consistent with PDI acting as an oxidant, PDI (CxxA)<sub>2</sub> did not support RNase A refolding (Fig. 4A). Surprisingly, PDI (CxxA)<sub>2</sub> was a dominant inhibitor of Ero1p-dependent oxidative folding, as inclusion of equimolar amounts of PDI (CxxA)<sub>2</sub> with wild-type PDI resulted in a severe reduction of RNase A reactivation (Fig. 4A). SDS-PAGE analysis revealed a disulfide cross-link between PDI (CxxA)<sub>2</sub> and Ero1p (Fig. 4B), suggesting that inhibition of refolding by PDI (CxxA)<sub>2</sub> resulted from sequestration of Ero1p via a disulfide cross-link between the two proteins. A similar cross-link is observed *in vivo* when both Ero1p and a mutant PDI are overexpressed, albeit at lower efficiency (20). Thus, a disulfide cross-link between PDI and Ero1p is likely to be an

obligatory intermediate during the oxidation of the PDI active sites by Ero1p.

What is the role of glutathione in oxidative protein folding in the ER? Cellular GSSG production increases with Ero1p activity (22). However, we found that Ero1p had no detectable activity as a direct oxidase of GSH to GSSG (16). Moreover, Ero1p-dependent folding of RNase A did not require glutathione, nor does disulfide formation *in vivo* (22). These considerations suggest that Ero1p-mediated oxidation of folding substrates proceeds by a protein-based relay that is largely independent of the bulk glutathione redox buffer (15). Consistent with this idea, Ero1p could efficiently drive oxidation of RNase A in the presence of a large excess of

reducing agent (1 or 2 mM GSH, Fig. 4C). During refolding, we then observed a gradual production of GSSG, which suggests that glutathione is not oxidized directly by Ero1p but rather by the reduction of Ero1p-derived disulfide bonds in PDI and/or substrates. Nonetheless, the glutathione buffer remained strongly reducing (e.g., at 20 min, GSH:GSSG  $\approx$  40:1) throughout the course of RNase A oxidation. These conditions were comparable to the reducing environment of the cytosol (6), where PDI at equilibrium should be largely reduced (23). Despite this, Ero1p- and PDI-driven oxidation of RNase A proceeded rapidly (within roughly a factor of 2 of the rate of oxidation without GSH) and PDI remained oxidized (16).

**Fig. 2.** Ero1p is a flavoprotein. **(A)** SDS-PAGE analysis of purified Ero1p-Py<sub>2</sub> either before or after further purification on an anti-polyoma column ( $\alpha$ -Py), with or without endoglycosidase H treatment, as indicated (15). No significant differences in oxidase activity or flavin-binding properties were observed between the proteins purified and not purified with anti-polyoma (16). **(B)** Purified Ero1p contains noncovalently bound FAD. Purified Ero1p from (A) was denatured and analyzed by rpHPLC coupled to a scanning fluorescence detector (15). The stoichiometry of bound oxidized FAD to Ero1p varied between 1:4 and 1:2. A fraction of Ero1p may have been misfolded or incapable of binding FAD. For comparison, a chromatogram of standards containing riboflavin, FMN, and FAD is shown (bottom trace).



REPORTS

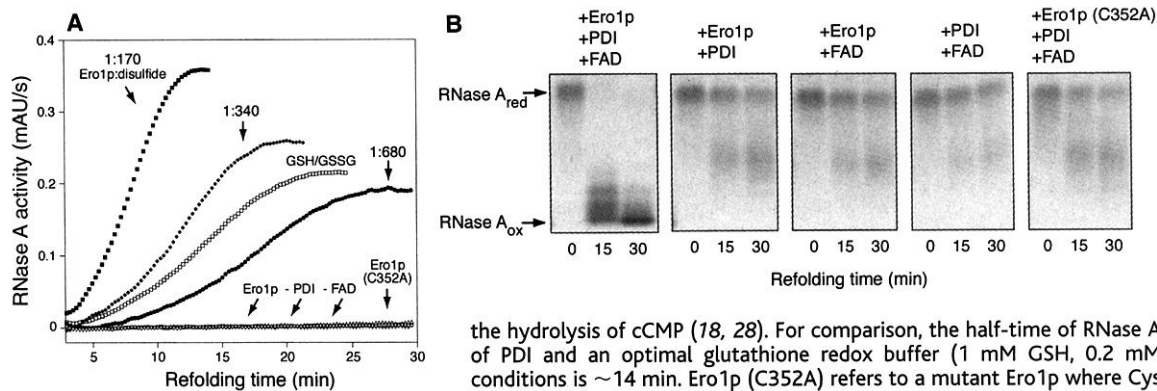


**Fig. 3.** Ero1p is a FAD-dependent oxidase. (A) Reconstitution of oxidative protein folding in vitro. The conversion of reduced RNase A (15  $\mu$ M) to its oxidized, active form in the presence or absence of Ero1p, PDI (0.9  $\mu$ M), and/or FAD (100  $\mu$ M) was assayed by monitoring

the hydrolysis of cCMP (18, 28). For comparison, the half-time of RNase A refolding in the presence of PDI and an optimal glutathione redox buffer (1 mM GSH, 0.2 mM GSSG) under the same conditions is  $\sim$ 14 min. Ero1p (C352A) refers to a mutant Ero1p where Cys<sup>352</sup> is changed to Ala. AU, absorbance units. (B) Direct observation of Ero1p-mediated catalysis of disulfide formation in RNase

**A.** Refolding of reduced RNase A (15  $\mu$ M) was followed in the absence or presence of Ero1p (0.36  $\mu$ M), PDI (0.9  $\mu$ M), and/or FAD (100  $\mu$ M) as indicated, quenched at the indicated times with AMS, and analyzed by nonreducing SDS-PAGE (28).

In summary, Ero1p is a FAD-dependent oxidase of PDI responsible for sustaining disulfide-linked protein folding in the ER. The FAD dependence of Ero1p is unexpected, because Ero1p contains no known flavin-binding motifs, and DsbB (which plays an analogous role to Ero1p in the bacterial periplasm) uses ubiquinone as the proximal oxidant in a flavin-independent reaction (4). Furthermore, unlike many microsome-associated flavoproteins, which face the cytosol,

Ero1p is localized within the ER lumen (15). Given the sensitivity of Ero1p-mediated oxidation to FAD levels, regulation of the amount of FAD available to Ero1p could play an important role in modulating oxidative folding in the ER.

Previous studies of disulfide bond formation in the ER often focused on the bulk redox potential of the organelle. In contrast, we have shown that oxidizing equivalents are delivered directly from Ero1p to folding sub-

strates via PDI, thereby allowing disulfide formation to occur rapidly even in a reducing environment. Accordingly, in vivo PDI is found predominantly in the oxidized form (20), contrary to predictions that the reduced form should be significantly populated if it were in equilibrium with the bulk ER redox buffer (1, 23). To support efficient disulfide-linked folding, the ER must simultaneously be able to rapidly add disulfide bonds to unfolded proteins and remove them from misfolded proteins. The shuttling of disulfide bonds through a protein relay, by largely insulating the Ero1p-driven oxidase machinery from other redox systems, could help to prevent Ero1p from interfering with the reduction or rearrangement of incorrect disulfides.

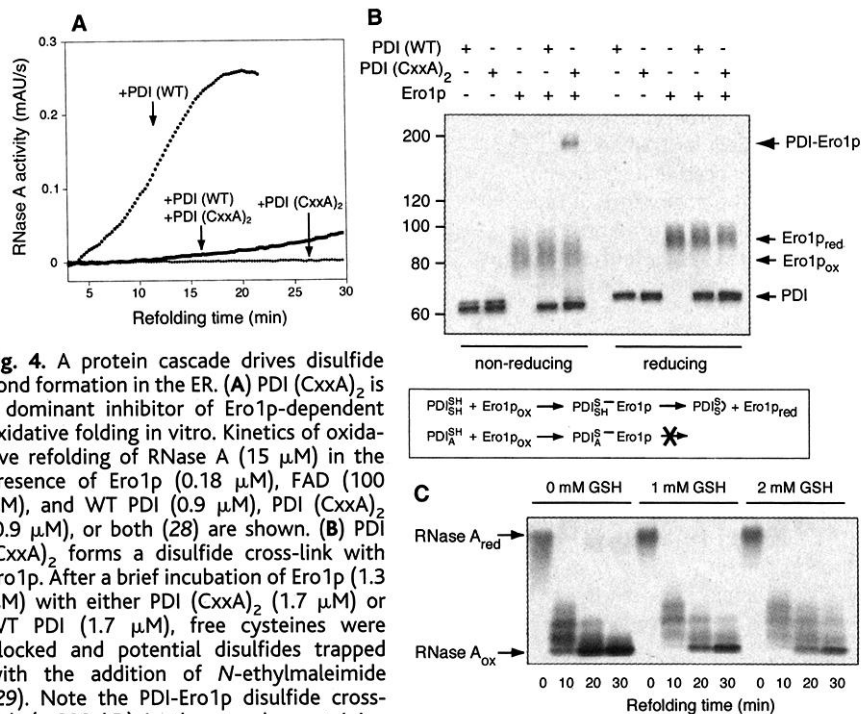


**Fig. 4.** A protein cascade drives disulfide bond formation in the ER. (A) PDI (CxxA)<sub>2</sub> is a dominant inhibitor of Ero1p-dependent oxidative folding in vitro. Kinetics of oxidative refolding of RNase A (15  $\mu$ M) in the presence of Ero1p (0.18  $\mu$ M), FAD (100  $\mu$ M), and WT PDI (0.9  $\mu$ M), PDI (CxxA)<sub>2</sub> (0.9  $\mu$ M), or both (28) are shown. (B) PDI (CxxA)<sub>2</sub> forms a disulfide cross-link with Ero1p. After a brief incubation of Ero1p (1.3  $\mu$ M) with either PDI (CxxA)<sub>2</sub> (1.7  $\mu$ M) or WT PDI (1.7  $\mu$ M), free cysteines were blocked and potential disulfides trapped with the addition of *N*-ethylmaleimide (29). Note the PDI-Ero1p disulfide cross-link ( $\sim$ 200 kD) in the sample containing Ero1p and PDI (CxxA)<sub>2</sub>. Western blot analysis confirmed the presence of both PDI and Ero1p in this band (16). Below, schematic model of Ero1p-catalyzed oxidation of PDI. PDI first forms a mixed disulfide with Ero1p, which is resolved by nucleophilic attack of the second cysteine in the PDI active site, yielding oxidized PDI. When the second cysteine is not present, the PDI-Ero1p cross-linked species cannot be readily resolved. (C) Ero1p can drive oxidative folding under reducing conditions. RNase A (15  $\mu$ M) refolding was initiated in the presence of Ero1p (0.36  $\mu$ M), PDI (0.9  $\mu$ M), FAD (100  $\mu$ M), and the indicated concentrations of reduced glutathione (GSH). At the specified times, disulfide content was monitored as described (28). The observed GSH:GSSG ratio (30) in the 2 mM GSH reactions at 10, 20, and 30 min was approximately 120:1, 40:1, and 17:1, respectively.

References and Notes

1. A. R. Frand, J. W. Cuozzo, C. A. Kaiser, *Trends Cell Biol.* **10**, 203 (2000).
2. A. Rietsch, J. Beckwith, *Annu. Rev. Genet.* **32**, 163 (1998).
3. T. Kobayashi et al., *Proc. Natl. Acad. Sci. U.S.A.* **94**, 11857 (1997).
4. M. Bader, W. Muse, D. P. Ballou, C. Gassner, J. C. Bardwell, *Cell* **98**, 217 (1999).
5. D. M. Ziegler, L. L. Poulsen, *Trends Biochem. Sci.* **2**, 79 (1977).
6. C. Hwang, A. J. Sinskey, H. F. Lodish, *Science* **257**, 1496 (1992).
7. M. G. Pollard, K. J. Travers, J. S. Weissman, *Mol. Cell* **1**, 171 (1998).
8. A. R. Frand, C. A. Kaiser, *Mol. Cell* **1**, 161 (1998).
9. J. C. Bardwell et al., *Proc. Natl. Acad. Sci. U.S.A.* **90**, 1038 (1993).
10. T. Stevens, B. Esmon, R. Schekman, *Cell* **30**, 439 (1982).
11. R. J. Barkovich et al., *J. Biol. Chem.* **272**, 9182 (1997).
12. W. W. Poon, T. Q. Do, B. N. Marbois, C. F. Clarke, *Mol. Aspects Med.* **18** (suppl.), S121 (1997).
13. A. M. Astin, J. M. Haslam, *Biochem. J.* **166**, 275 (1977).
14. G. Kispaal, P. Csere, C. Prohl, R. Lill, *EMBO J.* **18**, 3981 (1999).
15. See *Science Online* ([www.sciencemag.org/cgi/content/full/290/5496/1571/DC1](http://www.sciencemag.org/cgi/content/full/290/5496/1571/DC1)).
16. B. P. Tu, S. C. Ho-Schleyer, K. J. Travers, J. S. Weissman, unpublished data.
17. M. Wu, B. Repetto, D. M. Glerum, A. Tzagaloff, *Mol. Cell Biol.* **15**, 264 (1995).
18. M. M. Lyles, H. F. Gilbert, *Biochemistry* **30**, 613 (1991).
19. A. Cabibbo et al., *J. Biol. Chem.* **275**, 4827 (2000).
20. A. R. Frand, C. A. Kaiser, *Mol. Cell* **4**, 469 (1999).

21. M. C. Laboissiere, S. L. Sturley, R. T. Raines, *J. Biol. Chem.* **270**, 28006 (1995).
22. J. W. Cuozzo, C. A. Kaiser, *Nature Cell Biol.* **1**, 130 (1999).
23. J. Lundström, A. Holmgren, *Biochemistry* **32**, 6649 (1993).
24. J. L. Brodsky, S. Hamamoto, D. Feldheim, R. Schekman, *J. Cell Biol.* **120**, 95 (1993).
25. B. F. Horazdovsky, S. D. Emr, *J. Biol. Chem.* **268**, 4953 (1993).
26. We monitored disulfide content in substrates by SDS-PAGE analysis after modification with 4-acetamido-4'-maleimidylstilbene-2,2'-disulfonic acid (AMS), a thiol-modifying reagent that increases a protein's molecular weight by ~500 daltons per free thiol (3).
27. Microsomes were prepared as described and resuspended in Buffer 88 (24) containing 20 mM DTT for 1 hour, washed with Buffer 88 to remove DTT, and resuspended in Buffer 88 in the presence or absence of 200  $\mu$ M FAD. At the indicated times, aliquots were quenched with trichloroacetic acid (TCA) to 10% (w/v). TCA precipitates were resuspended in a solution of 1% SDS, 50 mM tris-Cl (pH 7.5), 1 mM phenylmethylsulfonyl fluoride, and 20 mM AMS, incubated at room temperature for 15 min and at 37°C for 10 min, and boiled for 2 min before Endo H treatment and SDS-PAGE analysis.
28. Oxidative refolding was initiated by addition of reduced RNase A (18) to the indicated concentration of purified Ero1p (15), bacterially expressed PDI (15), and/or FAD (100  $\mu$ M) in a buffer containing 18 mM cytidine 2',3'-cyclic monophosphate (cCMP), 0.1 M tris-acetate (pH 8.0), 65 mM NaCl, 2 mM EDTA, and 0.005% digitonin. RNase A activity (hydrolysis of cCMP) was assayed by monitoring the rate of change of absorbance at 296 nm at 25°C (18). The disulfide content of RNase A was monitored in a similar buffer, but without cCMP. Samples were analyzed at the indicated times by the addition of SDS-PAGE buffer and 10 mM AMS, incubation for 30 min at room temperature, followed by nonreducing SDS-PAGE.
29. Reduced wild-type PDI or PDI (CxxA)<sub>2</sub> (1.7  $\mu$ M) was added to Ero1p (1.3  $\mu$ M) in a buffer containing 50 mM Hepes (pH 7.5), 100 mM NaCl, 2 mM EDTA, and 0.05% digitonin. After 10 min at room temperature, free sulfhydryls were quenched by addition of SDS-PAGE buffer and 10 mM *N*-ethylmaleimide for 1 hour. The sample was then divided in two and subjected to SDS-PAGE under reducing or nonreducing conditions.
30. M. E. Anderson, *Methods Enzymol.* **113**, 548 (1985).
31. We thank C. Kaiser, R. Lill, E. O'Shea, T. Stevens, and J. Winther for strains and antibodies and W. Lim, S. Miller, E. O'Shea, P. Ortiz de Montellano, and members of the Weissman laboratory for helpful discussions. Supported by NIH, the Searle Scholars Program, the David and Lucile Packard Foundation, and an Howard Hughes Medical Institute predoctoral fellowship (B.P.T.).

14 August 2000; accepted 20 October 2000

## $\beta$ -Arrestin 2: A Receptor-Regulated MAPK Scaffold for the Activation of JNK3

Patricia H. McDonald,<sup>1\*</sup> Chi-Wing Chow,<sup>2\*</sup>  
William E. Miller,<sup>1\*</sup> Stéphane A. Laporte,<sup>3</sup> Michael E. Field,<sup>1</sup>  
Fang-Tsyr Lin,<sup>1</sup> Roger J. Davis,<sup>2</sup> Robert J. Lefkowitz<sup>1†</sup>

$\beta$ -Arrestins, originally discovered in the context of heterotrimeric guanine nucleotide binding protein-coupled receptor (GPCR) desensitization, also function in internalization and signaling of these receptors. We identified c-Jun amino-terminal kinase 3 (JNK3) as a binding partner of  $\beta$ -arrestin 2 using a yeast two-hybrid screen and by coimmunoprecipitation from mouse brain extracts or cotransfected COS-7 cells. The upstream JNK activators apoptosis signal-regulating kinase 1 (ASK1) and mitogen-activated protein kinase (MAPK) kinase 4 were also found in complex with  $\beta$ -arrestin 2. Cellular transfection of  $\beta$ -arrestin 2 caused cytosolic retention of JNK3 and enhanced JNK3 phosphorylation stimulated by ASK1. Moreover, stimulation of the angiotensin II type 1A receptor activated JNK3 and triggered the colocalization of  $\beta$ -arrestin 2 and active JNK3 to intracellular vesicles. Thus,  $\beta$ -arrestin 2 acts as a scaffold protein, which brings the spatial distribution and activity of this MAPK module under the control of a GPCR.

$\beta$ -Arrestins bind to  $\beta_2$ -adrenergic receptors ( $\beta_2$ ARs) after the receptors have been phosphorylated by guanine nucleotide binding protein (G protein)-coupled receptor kinases (GRKs), thereby interdicting further signal transduction to heterotrimeric G proteins (1). Once viewed as involved exclusively in receptor desensitization,  $\beta$ -arrestins are now known to act as adaptors to facilitate clathrin-mediated endocytosis of certain members of the GPCR family (2, 3). They also recruit

activated c-Src into complexes with the  $\beta_2$ AR, which appears to be involved in activation of extracellular signal-regulated kinases (ERK1 and ERK2) (4-6).

In mammalian cells, at least three groups of mitogen-activated protein kinases (MAPKs) have been identified: the ERKs (1 and 2), the p38 protein kinases ( $\alpha$ ,  $\beta$ ,  $\gamma$ , and  $\delta$ ), and the c-Jun NH<sub>2</sub>-terminal kinases (JNKs; also referred to as stress-activated protein kinases or SAPKs) (7). The JNKs are encoded by at least three genes (JNK1, -2, and -3), and the transcripts of each of these genes are alternatively spliced to create mRNAs that encode 46- and 54-kD JNK isoforms (8). Moreover, JNK activity is increased in settings of cell stress, mitogenesis, differentiation, morphogenesis, and apoptosis (7, 9).

JNK is activated by dual phosphorylation on threonine and tyrosine residues catalyzed by a MAPK kinase (such as MKK4 or MKK7), which, in turn, is phosphorylated

and activated by a MAPKK kinase (such as MEKK1, MLK, or ASK1). The functional integrity of each MAP kinase cascade is thought to be established by specific molecular interactions both between the kinases and cytoplasmic scaffolds or anchor proteins (10).

MAPK pathways are activated by GPCRs, including m1 and m2 muscarinic and angiotensin II type 1A (AT1A) receptors (11, 12) and by growth factor receptors with intrinsic tyrosine kinase activity. Here we report the identification of  $\beta$ -arrestin 2 as a binding partner of JNK3 and describe a GPCR-regulated MAPK module wherein  $\beta$ -arrestin 2 functions as a scaffold protein.

To identify novel binding partners of  $\beta$ -arrestin 2, we used the yeast two-hybrid system based on a GAL4- $\beta$ -arrestin 2 fusion protein to screen a rat brain cDNA library (13). Three positive clones were obtained, two of which encoded fusion proteins of the GAL4 activation domain with a COOH-terminal portion of JNK2 and one that encoded a COOH-terminal portion of the JNK3 isoform (14). All three clones encoded p54 splice variants of JNK. These interactions were confirmed by cotransforming yeast strain pJ69-4A with pAS2-1- $\beta$ -arrestin 2 and the JNK clones (ct-JNK2 and ct-JNK3) obtained from the yeast two-hybrid screen. pAS2-1- $\beta$ -arrestin 1 also interacted with both ct-JNK clones in the same assay. However, yeast transformed with pAS2-1- $\beta$ -arrestin 1 and either ct-JNK2 or ct-JNK3 grew more poorly than those transformed with pAS2-1- $\beta$ -arrestin 2 and either ct-JNK clone. The  $\beta$ -arrestins did not interact in the yeast two-hybrid system with the GAL4 activation domain encoded by pGAD10, nor did the ct-JNK clones interact with the GAL4 DNA binding domains encoded by pAS2-1 or with pAS2-1-Lamin, suggesting that the interactions of  $\beta$ -arrestins with the ct-JNKs are specific (14).

To determine whether the endogenous proteins interact,  $\beta$ -arrestin was immunoprecipitated from mouse brain extract with a  $\beta$ -arres-

<sup>1</sup>Howard Hughes Medical Institute and Departments of Medicine, Cardiology, and Biochemistry, Duke University Medical Center, Box 3821, Durham, NC 27710, USA. <sup>2</sup>Howard Hughes Medical Institute and Program in Molecular Medicine, Department of Biochemistry and Molecular Biology, University of Massachusetts Medical School, Worcester, MA 01605, USA. <sup>3</sup>Department of Cell Biology, Duke University Medical Center, Box 3287, Durham, NC 27710, USA.

\*These authors contributed equally to this work.

†To whom correspondence should be addressed.